FERMILAB-PUB-24-0429-STUDENT

Signal discrimination for neutron-antineutron oscillation sensitivity study at DUNE

Justin Wheeler[1, a)]
Fermilab

(Dated: 1 August 2024)

The Deep Underground Neutrino Experiment (DUNE) aims to measure neutrino oscillations as well as search for beyond the standard model physics such as baryon number violating (BNV) processes. DUNE will use a 70 kt Liquid Argon Time Projection Chamber (LArTPC) located more than 1 km underground. A promising BNV process is neutron-antineutron oscillation ($n \to \bar{n}$) which, if discovered, would offer unique insight into the baryon asymmetry of the universe. We are developing a classification algorithm that separates $n \to \bar{n}$ events from major background atmospheric neutrino interactions using DUNE far detector simulations. We will perform the classification of signals and backgrounds by analyzing key features such as the multiplicity, isotropy, and kinematics of the reconstructed events. In the future, this algorithm can be used to obtain the sensitivity of the DUNE detectors to the neutron-antineutron oscillation lifetime.

I. INTRODUCTION

The present baryon asymmetry of the universe points indirectly towards the existence of baryon number violating (BNV) processes given Sakharov's conditions[1]. BNV processes that probe physics beyond the Standard Model (SM) are classified by their change in baryon number (ΔB). One such process is neutron-antineutron oscillation ($n \to \bar{n}$) with $\Delta B = 2$. This process is the spontaneous conversion of a neutron to an antineutron with the same energy and momentum[2].

There have been a number of previous experiments searching for $n \to \bar{n}$ in both free neutrons[3] and bound neutrons[4–10], none of which have observed a statistically significant signal. Although, through these efforts, constraints on the $n \to \bar{n}$ oscillation time have been set at $\tau_{n\to\bar{n}} > 0.86 \times 10^8$ s for free neutron oscillation[3] and at $\tau_{n\to\bar{n}} > 4.7 \times 10^8$ s for bound neutrons[10].

Experimental searches for $n \to \bar{n}$ rely on observing particles produced when a neutron spontaneously converts to an antineutron and annihilates with a nearby nucleon. These signal events, $n \to \bar{n}$, need to be observed with certainty to place limits on the $n \to \bar{n}$ lifetime. Observation of these interactions are obscured by the dominant source of background, atmospheric neutrino interactions. Thus, classification algorithms must be developed to reject background events, maintain signal events, and quantify the signal and background efficiencies.

In this paper we present an algorithm that can be applied to estimate the sensitivity of the DUNE far detector to $n \to \bar{n}$ oscillation. The algorithm is trained on simulated atmospheric neutrino and $n \to \bar{n}$ events within the Deep Underground Neutrino Experiment (DUNE) far detector horizontal drift module.

[a)]Also at Carthage College

II. THE DEEP UNDERGROUND NEUTRINO EXPERIMENT

DUNE will be a world-class neutrino experiment and nucleon decay detector. The experiment is slated to measure several neutrino oscillation parameters and probe physics beyond the SM. With Liquid Argon Time Projection Chamber (LArTPC) technology, DUNE will measure neutrinos at a near detector and 1300 km away at a far detector. This far detector, more than 1 km underground, is protected from cosmic rays by the earth, and thus is ideal for the $n \to \bar{n}$ oscillation search.

DUNE far detector consists of 70 ktons of liquid argon with 40 kton of fiducial volume. This study considers a $n \to \bar{n}$ oscillation search for 10 yrs leading to a total exposure of 400 kton·yrs. The bound neutrons serve as the neutrons used in the $n \to \bar{n}$ oscillation search with DUNE.

Within the TPC, an oscillated antineutron will annihilate with a nearby nucleon within the argon nucleus, producing many pions and other charged particles. These charges particles ionize nearby argon to produce electrons. These electrons drift in the electric field, then induce and deposit charge at the anode planes.

III. SENSITIVITY CALCULATION

A detector's sensitivity can be calculated with a given exposure, signal selection efficiency, and expected background rate. The expected sensitivity is derived with a 90% confidence level for bound neutrons. Then, the lifetime sensitivity for a free neutron is calculated using the conversion from nucleus-bound neutron to free neutron oscillation[11]. It is important to note that the sensitivity calculation outlined in this section does not take into account systematic uncertainty.

The Bayesian statistical method is used to express conditional probability when there is a given observation. The probability of event A given event B is

$$P(A|B) = \frac{P(B|A)P(A)}{P(B)}, \tag{1}$$

where $P(A)$ and $P(B)$ are individual probabilities of A and B. The occurrence of events follows a Poisson distribution

$$p(n,\lambda) = \frac{e^{-\lambda}\lambda^n}{n!}, \tag{2}$$

where n is the number of observed events and λ is the mean of the distribution corresponding to an expected event rate. With the DUNE far detector we will observe a number of events n_{obs} given the truth-level variable $n_s + n_b$ which is the sum of the true number of observed signal events and the theorized background rate at the detector. This probability follows the Poisson distribution

$$P(n_{\mathrm{obs}}|n_s + n_b) = p(n_{\mathrm{obs}}, n_s + n_b). \tag{3}$$

Applying Bayes' theorem to rearrange terms to yield an equation that can be used to find the true number of signal events,

$$\begin{aligned} P(n_{\mathrm{obs}}|n_s + n_b)P(n_s + n_b) &= P(n_s + n_b|n_{\mathrm{obs}})P(n_{\mathrm{obs}}), \\ P(n_{\mathrm{obs}}|n_s + n_b) &= P(n_s + n_b|n_{\mathrm{obs}})P(n_{\mathrm{obs}}), \end{aligned} \tag{4}$$

where we set $P(n_s + n_b)$ equal to 1 because we are not taking systematic uncertainties into account in this analysis. For the $n \to \bar{n}$ oscillation lifetime sensitivity, no observation of signal events are hypothesized, in other words the number of observed events is set equal to the background rate. The lifetime sensitivity to 90% confidence level of the $n \to \bar{n}$ oscillation process is found by evaluating n_s to the point where the integral of eq. (4) makes 90% of the integral over the entire n_s domain

$$0.9 = \frac{\int_0^{\bar{n_s}} P(n_{\mathrm{obs}}|n_s + n_b)}{\int_0^{\infty} P(n_{\mathrm{obs}}|n_s + n_b)}, \tag{5}$$

where $\bar{n_s}$ is our 90% confidence limit for the number of signal events observed. The 90% C.L. for the rate of events $\Gamma_{0.9}$ can then be calculated

$$\Gamma_{0.9} = \frac{\bar{n_s}}{E\varepsilon}, \tag{6}$$

where E is the exposure of the DUNE far detector and ε is the signal selection efficiency of our classifier. Next, the 90% C.L. limit for the $n \to \bar{n}$ oscillation lifetime of bound neutrons $T_{n\to\bar{n}}$ is defined as

$$T_{n\to\bar{n}} = \frac{1}{\Gamma_{0.9}}. \tag{7}$$

Finally, the free $n \to \bar{n}$ oscillation lifetime $\tau_n \to \bar{n}$ is related to the bound $n \to \bar{n}$ oscillation lifetime by the nuclear suppression factor R by

$$\tau_n \to \bar{n}^2 = \frac{T_{n\to\bar{n}}}{R}. \tag{8}$$

The suppression factor varies for different nuclei. Recently, the suppression factor for argon-40 nuclei was calculated[12] to be 5.6×10^{22} s^{-1}. The preliminary sensitivity in DUNE without systematic uncertainty analysis is calculated using this value.

IV. METHODS

This analysis uses 100k simulated signal and background events. The simulations were performed using GENIE 3.4.0 (model: hn BR) as the generator. The simulation software used is DUNEsw: v09_85_00d00 within the far detector horizontal drift module with dimensions 1x2x6 m. Additionally, modeling of the atmospheric neutrino events was performed with a larger than realistic flux of low-energy neutrinos. In the future, these can be reweighted, but remain unweighted for the purposes of this analysis.

These events are then processed in two stages, first applying simple analysis cuts before applying a Boosted Decision Tree (BDT) technique to extract the signal.

A. Analysis precuts

Based on several distinct features of the signal and background events, several preliminary cuts are applied to reduce background and maintain high signal efficiency. We reject all events with less than 1 reconstructed particle, which is defined as a reconstructed track-like or shower-like object, as all signal events will produce one or more particles in the annihilation process and very few produce exactly one. Next, we reject all events with greater than 1.8 GeV total visible energy and less than 980 MeV/c total momentum. Neutrons and protons have a rest mass of $\sim$940 MeV/c^2, so the annihilation of $\bar{n}n$ and $\bar{n}p$ will likely produce a visible energy at or below 1.8 GeV, leaving only background events producing visible energies above this threshold. After the cuts on multiplicity and kinematics, we retain 94.23% of our signal and reject 62.93% of the background.

B. Feature variables

The feature variables used in this analysis can be divided into three categories: multiplicity, kinematics, and isotropy. All variables fed into the classification algorithm are shown in fig. 1.

The multiplicity variables used are the number of reconstructed track-like objects, shower-like objects, protons, and muons. Tracks and showers were clustered and classified by the Pandora algorithm[13]. Particles were identified[14] using a metric called PIDA[11]. This metric is calculated from the fact that for a given point on a reconstructed track, $\frac{dE}{dx}$ can be found at the point, as well as the residual length R from the point to the end of the track. PIDA is defined as the median of all track points i for which the residual range R_i is less than 30 cm

$$PIDA = \left\langle \left(\frac{dE}{dx}\right)_i R_i^{0.42} \right\rangle. \tag{9}$$

A plot showing the distribution of calculated PIDA for various truth-level particle types is shown in fig. 2. All particles with PIDA greater than 10 are classified as protons and the rest are classified as muons.

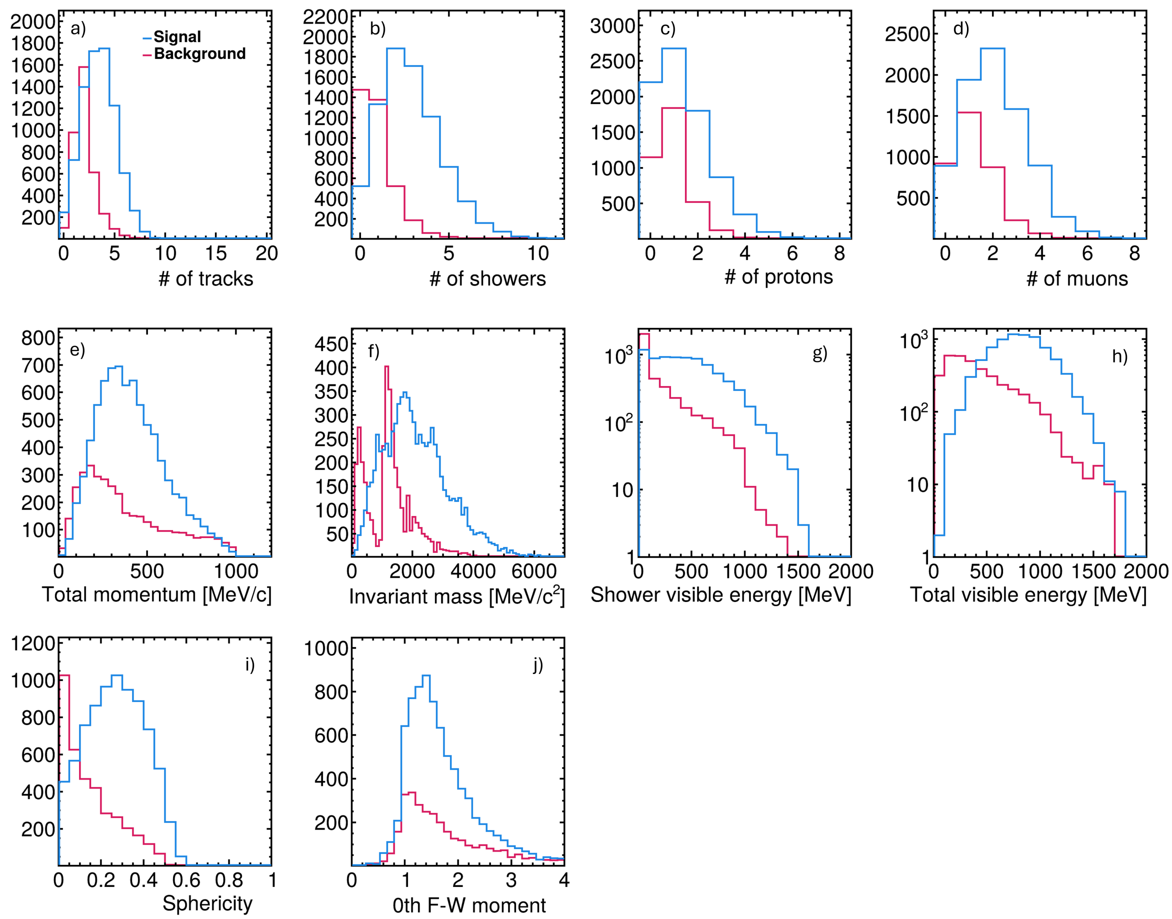

FIG. 1. Histograms of the 10 feature variables used to train the classifier for signal (blue) and background (red). These histograms were generated with a subsample of 10k events and the background data has not been flux weighted yet. All data shown is reconstructed from Pandora, a reconstruction algorithm

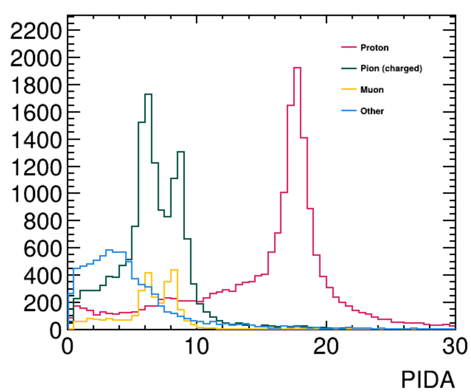

FIG. 2. Distribution of calculated PIDA metric from reconstructed variables for truth-level protons, pions, muons, and other.

The kinematic variables are reconstructed total momentum, invariant mass, total visible energy, and visible energy from shower-like objects.

The isotropy variables used are sphericity and the 0-th order Fox-Wolfram moment. Sphericity, related to how spread out the directions of the product particles are is calculated through the eigenvalues of the sphericity tensor for an event. The sphericity tensor is defined as follows

$$S^{\alpha\beta} = \frac{\sum_i p_i^{\alpha} p_i^{\beta}}{\sum_i p_i^2}, \tag{10}$$

where $\sum_i$ runs over all particles in the event, p_i is the momentum of the i-th particle, and α and β run over all spatial directions x, y, and z. The eigenvalues $\lambda_1, \lambda_2, \lambda_3$ can be calculated, ordered, and normalized such that $\lambda_1 > \lambda_2 > \lambda_3$ and $\lambda_1 + \lambda_2 + \lambda_3 = 1$. The sphericity of an event, F_{spher}, is defined as

$$F_{\text{spher}} = \frac{3}{2}(\lambda_2 + \lambda_3). \tag{11}$$

The Fox-Wolfram moments are another measure of the spread of final-state particles in an event represented by H_l with $l =$

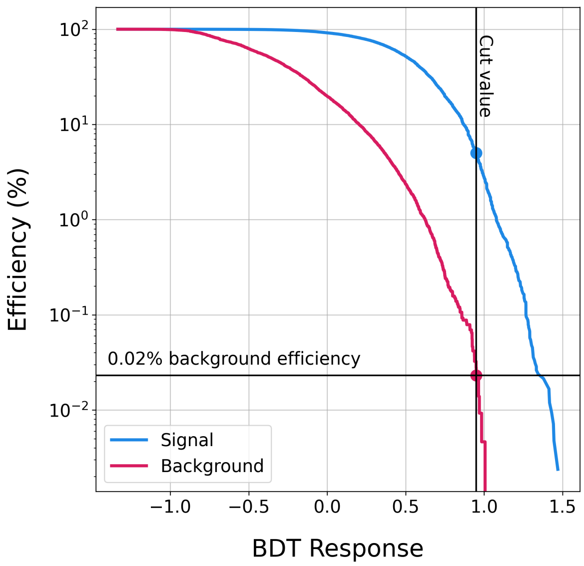

FIG. 3. Signal (blue) and background (red) as a function of Boosted Decision Tree response. The vertical black line indicates the cut point which is determined at the response at which 0.02% background efficiency is attained.

$0, 1, 2...$ is defined by[15]

$$H_l = \sum_{i,j} \frac{|\boldsymbol{p}_i||\boldsymbol{p}_j|}{E_{\text{vis}}^2} P_l(\cos\theta_{ij}) . \quad (12)$$

where θ_{ij} is the opening angle between particles i and j, and Evis is the total visible energy of the event recorded from calorimetry by the TPC wire planes. Finally, the $P_l(x)$ are the Legendre polynomials.

V. PRELIMINARY RESULTS

Placing a cut at 99.98% background rejection (0.02% background efficiency) we obtain a signal efficiency of 5.01% shown in fig. 3. This corresponds to a the 90% C.L. free $n \to \bar{n}$ oscillation lifetime limit of 6.67×10^8 s following the procedure outlined in section III. This lifetime limit was calculated without systematic uncertainty analysis, and serves as a preliminary estimate for how effective the classification algorithm might be given proper particle identification and systematic uncertainty analysis.

VI. DISCUSSION

We have produced a classification algorithm that yields a 5.01% signal efficiency at a 99.98% background rejection probability. The 90% C.L. free $n \to \bar{n}$ oscillation lifetime limit of 6.67×10^8 s was derived at this cut and was determined without systematic uncertainty analysis. As a comparison, a previous study utilizing both BDT and a convolution neural network at the same background rejection probability yielded a signal efficiency of 8.0%[16]. We made the assumption that there were no uncertainties in the far detector exposure, and signal and background efficiency. There remains methods of improving the signal efficiency of this algorithm through avenues of tuning BDT parameters to prevent over-training, experimenting with different input feature variables, and optimizing an analysis cut towards best sensitivity. Finally, with future research, flux re-weighting can be performed on the background signal to yield more accurate atmospheric neutrino interactions, and as particle identification with DUNE progresses, multiplicity variables will become more accurate.

[1] A. D. Sakharov, "Violation of cp in variance, c asymmetry, and baryon asymmetry of the universe," Usp. Fiz. Nauk **161**, 61–64 (1991).

[2] S. Gardner and X. Yan, "Phenomenology of neutron-antineutron conversion," Physical Review D **97** (2018), 10.1103/physrevd.97.056008.

[3] M. B.-C. et al., "A new experimental limit on neutron-antineutron oscillations," Usp. Fiz. Nauk **63**, 409–416 (1994).

[4] K. A. et al. (Super-Kamiokande Collaboration), "Search for $n-\bar{n}$ oscillation in super-kamiokande," Phys. Rev. D **91**, 072006 (2015).

[5] B. A. et al. (SNO Collaboration), "Search for neutron-antineutron oscillations at the sudbury neutrino observatory," Phys. Rev. D **96**, 092005 (2017).

[6] J. C. et al., "Search for neutron-antineutron oscillations using multiprong events in soudan 2," Phys. Rev. D **66**, 032004 (2002).

[7] M. T. et al., "Search for neutron-antineutron oscillation in ^{16}O nuclei," Phys. Rev. D **34**, 902–904 (1986).

[8] T. W. J. et al (Irvine-Michigan-Brookhaven Collaboration), "Search for $n-\bar{n}$ oscillation in oxygen," Phys. Rev. Lett. **52**, 720–723 (1984).

[9] C. B. et al., "Search for neutron-antineutron oscillations in the fréjus detector," Physics Letters B **240**, 237–242 (1990).

[10] K. A. et al. (Super-Kamiokande Collaboration), "Neutron-antineutron oscillation search using a 0.37 megaton-years exposure of super-kamiokande," Phys. Rev. D **103**, 012008 (2021).

[11] Y.-j. Jwa, *Searching for Clues for a Matter Dominated Universe in Liquid Argon Time Projection Chambers*, Ph.D. thesis, Columbia U. (2022).

[12] J. L. Barrow, E. S. Golubeva, E. Paryev, and J.-M. Richard, "Progress and simulations for intranuclear neutron-antineutron transformations in $^{40}_{18}$Ar," Phys. Rev. D **101**, 036008 (2020).

[13] T.-J. Yang (DUNE), "Automated Reconstruction, Signal Processing and Particle Identification in DUNE," PoS **ICHEP2016**, 183 (2016).

[14] J. S. Marshall and M. A. Thomson, "The pandora software development kit for pattern recognition," The European Physical Journal C **75**, 439 (2015).

[15] G. C. Fox and S. Wolfram, "Observables for the analysis of event shapes in e^+e^- annihilation and other processes," Phys. Rev. Lett. **41**, 1581–1585 (1978).

[16] e. a. B. Abi, "Deep underground neutrino experiment (dune), far detector technical design report, volume ii: Dune physics," (2020), arXiv:2002.03005 [hep-ex].